

Purity Monitor Studies in Medium Liquid Argon TPC

I. Badhrees

Abstract—This paper is an attempt to describe some of the results that had been found through a journey of study in the field of particle physics. This study consists of two parts, one about the measurement of the cross section of the decay of the Z particle in two electrons, and the other deals with the measurement of the cross section of the multi-photon absorption process using a beam of Laser in the Liquid Argon Time Projection Chamber.

The first part of the paper concerns the results based on the analysis of a data sample containing 8120 ee candidates to reconstruct the mass of the Z particle for each event where each event has an ee pair with $PT_{(e)} > 20\text{GeV}$, and $\eta_{(e)} < 2.5$. Monte Carlo templates of the reconstructed Z particle were produced as a function of the Z mass scale. The distribution of the reconstructed Z mass in the data was compared to the Monte Carlo templates, where the total cross section is calculated to be equal to 1432pb.

The second part concerns the Liquid Argon Time Projection Chamber, LAr TPC, the results of the interaction of the UV Laser, Nd-YAG with $\lambda = 266\text{mm}$, with LAr and through the study of the multi-photon ionization process as a part of the R&D at Bern University. The main result of this study was the cross section of the process of the multi-photon ionization process of the LAr, $\sigma_e = 1.24 \pm 0.10 \text{stat} \pm 0.30 \text{sys} \cdot 10^{-56} \text{cm}^4$.

Keywords—ATLAS, CERN, KACST, LArTPC, Particle Physics.

I. INTRODUCTION

PARTICLE physics is the branch of physics that deals with matter and its interactions. Particle physics is the study of the basic elements of matter and the forces acting among them. It aims to determine the fundamental laws that control the makeup of matter and the physical universe. It is also referred to as “High Energy Physics” because many elementary particles do not occur under normal circumstances in nature, but can be created and detected.

From the very beginning and since the creation of mankind, people questioned the universe posing the question: “What is the universe made of?” To answer this question a model known as the Standard Model (SM) [1], established in the late 70’s. The SM of particle physics describes the constituents of matter and the interactions among them. The constituents of matter are called fermions, (possessing half integer spin), while the particles responsible for their interactions are called bosons, (possessing integer spin). This model consists of three generations of particles, quarks, and leptons. Physicists have identified 12 building blocks divided into 6 quarks and 6 leptons [2], these are the fundamental constituents of matter.

I Badhrees is with King Abdulaziz City for Science and Technology, Riyadh, KSA (phone: 00966 505 555 1727; e-mail: ibadhrees@kacst.edu.sa).

See Fig. 1.

Beside the fundamental particles in the SM, scientists distinguish four elementary types of forces acting among particles: Strong, Weak, Electromagnetic, and Gravitational forces [3], see Table I [4]. Particles transmit forces among each other by exchanging force-carriers, which are referred to as bosons, which carry discrete amounts of energy called quanta from one particle to another.

The Z bosons are the mediators of the weak interactions, predicted by Glashow, Salaam, and Weinberg in 1968. The idea that the weak interaction is mediated by very heavy exchange bosons was accepted before they were discovered. The structure of the Fermi theory of β -decay implies that the interaction is point like, which implies that the exchange bosons have to be heavy. This was confirmed when W and Z bosons were detected experimentally and their properties could be measured. The Z boson’s properties imply a mixing of the electromagnetic and weak interactions. In this part of the paper, the measurement of the cross section of the Z particle decaying into two electrons is shown.

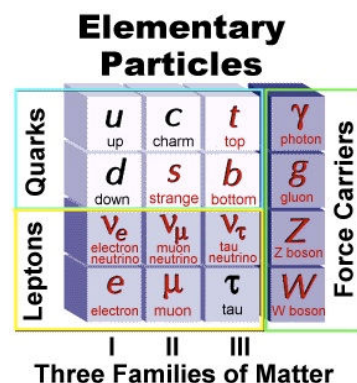


Fig. 1 The Particles of the Standard Model organized into Quarks, Leptons

The first part of the measurement took place at CERN, the European organization for Nuclear Research, at the ATLAS experiment [5], a Toroidal LHC Apparatus. In 1991 a historical decision was made to build and operate the world’s largest and most powerful accelerator in the world, the Large Hadron Collider [6], LHC, Fig. 2. The LHC is a particle accelerator with a 27 km circumference that hosts a number of experiments. This accelerator collides two bunches of protons to reach an energy of up to 14 TeV. The goals of the LHC are plentiful, one of these goals is to discover the source of the symmetry breaking: the Higgs boson, and for that reason Prof.

Petter Higgs received the Nobel Prize of physics that year (2013). In addition, one of the major physics topics to be investigated at the LHC is the search for super-symmetric (SUSY) particles, which should have a large cross-section at TeV scale energies. Other topics for new physics include studies of quark compositions, leptons, quarks and heavy vector bosons. One of the largest experiments on the LHC ring is the ATLAS experiment, Fig. 3. It is a general-purpose particle physics experiment that will explore the fundamental nature of matter and the basic forces that shape our universe. This detector is a 46m long, 25m wide, 25m high, and weighs 7000 tons. This detector has several goals: to provide an excellent electromagnetic calorimetric for electron and photon measurement and identification, efficient tracking of leptons, and good muon identification and momentum resolution.

This detector consists of different parts, the Inner Detector, Electromagnetic Calorimeter, Hadron Calorimeter, and Muon Spectrometer.

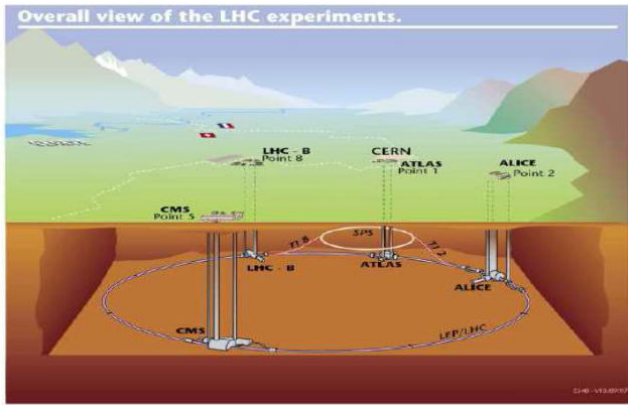


Fig. 2 The Large Hadron Collider

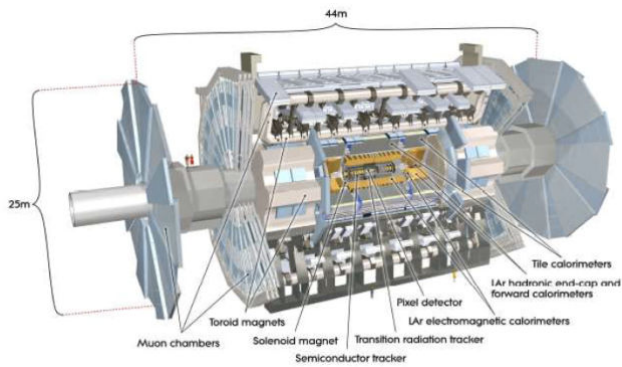


Fig. 3 ATLAS experiment

The second part of this paper will discuss the R&D of novel detector for the detection of neutrinos, precisely, the Liquid Argon Time Projection Chamber, LAr TPC.

A neutrino is a neutral particle with a half-integral spin; thus, it is fermions. According to the Standard Model, we have three flavors of the neutrinos associated with the three leptons which are, electrons, muons and taus [7].

In addition, the neutrino interacts via weak charges and neutral currents, electromagnetic and gravitational forces but not strong interactions. Neutrinos are interesting for studies in the field of particle physics as well as cosmology and astrophysics, since they are able to explain the hypothesis of the nuclear energy generated in the Sun and in the stars. At the same time, neutrinos are difficult in terms of detection because they interact weakly with matter meaning they have a small cross-section.

According to Beth and Peierls [8], the predicted strength of the weak interaction would allow a neutrino to pass through 80 billion kilometers of water without interacting, with a cross-section about 10^{-38} , as a consequence it seems it would be impossible to detect. Thus, enormous flux of neutrinos and large targets typically hundreds or thousands tons of material are essential and required to detect neutrinos. Recent neutrino oscillation data provides evidence that neutrino species have non-zero masses. As a result, a number of theoretical and phenomenological issues appear in the domain of the neutrinos, which is a step forward to the studies beyond the Standard Model. Neutrino mixing and oscillations are two important issues that occur during the time evolution of the neutrinos.

Moreover, neutrino oscillation is the present explanation of massive neutrinos that come from oscillation experiments. The first introduction of the neutrino oscillation is dated back to 1957 and B. Pontecorvo [9] [10], when he first proposed mixing between neutrinos and anti-neutrinos.

Another distinguishing feature of massive neutrinos is the possibility of the decay of a member from one "flavor" to another, which may lead to many interesting new phenomena in the laboratory as well as the cosmological field [11]. In 1962, Z. Maki, M. Nakagawa, and S. Sakata (MNS) proposed the mixing between generations of neutrinos that we know today [12]. This mixing is described through the following MNS matrices:

$$\begin{pmatrix} 1 & 0 & 0 \\ 0 & c_{23} & s_{23} \\ 0 & -s_{23} & c_{23} \end{pmatrix} \begin{pmatrix} c_{13} & 0 & s_{13}e^{-i\delta} \\ 0 & 1 & 0 \\ -s_{13}e^{i\delta} & 0 & c_{13} \end{pmatrix} \begin{pmatrix} c_{12} & s_{12} & 0 \\ -s_{12} & c_{12} & 1 \\ 0 & 0 & 1 \end{pmatrix}$$

where $c_{ij} = \cos\theta_{ij}$, $s_{ij} = \sin\theta_{ij}$ ($i, j = 1, 2, 3$ are the generation indices), and δ is the CP violating phase. In this parameterization, the mixing angles are θ_{12} , θ_{13} and θ_{23} . The first matrix represents ν_μ to ν_τ the second ν_e to ν_μ mixing and the third ν_e to ν_μ mixing. E is the energy of the neutrino.

The probability of the oscillation taking place where the neutrino changes its flavor is given by:

$$P_{\alpha \rightarrow \beta} = \left| \langle \nu_\beta | \nu_\alpha \rangle \right|^2 = \sin^2 2\theta \sin^2 \frac{1}{2} (E_2 - E_1) t \quad (1)$$

This formula is held under the assumption of oscillation taking place between two families of neutrinos assuming that $E_i \gg m_i$, thus:

$$P_{\alpha \rightarrow \beta} = \left| \langle \nu_\beta | \nu_\alpha \rangle \right|^2 = \sin^2 2\theta \sin^2 1.27 \left(\frac{\Delta m^2 L}{E} \right) t \quad (2)$$

Consequently, for the detection of these particles we need to build massive detectors, installed underground in order to be shielded from cosmic rays and environmental radioactivity sources. In this context, different technologies have been used for the studies of neutrino interactions and oscillations, among them is the SAGE experiment [13], Kamiokande [14] and the Super Kamiokande collaborations [15] [16], SNO [17], CHOOZ experiment [18], Mini-BooNE [19].

The Liquid Argon Time Projection Chamber LAr TPC is another promising technique in the detection of neutrinos. In 1977, this detector was proposed by Carlo Rubbia, where he wanted to merge the superb capability of imaging of the bubble chamber with electronic readouts in one device [20]. ICARUS is a pioneering effort exploiting this technique [21]; it has been installed at Gran Sasso Laboratory, LNGS, Italy. This part of the paper will revolve around one of the three detectors located at Elbert Einstein Institute and precisely in the Laboratory of High Energy Physics, LHEP. This detector is the Medium sized detector, with 30cm drift distance. In addition, the result of the measurement of the purity, recombination, and the cross section of the multi-photon ionization of LAr in the study of the UV [22] laser beam as a mean calibration of the detector will be shown.

A Time Projection Chamber is a detector, which measures the ionization produced by the passage of a charge particle in a given volume. It is a wire chamber consisting of two electrodes, the cathode and an anode that are immersed in a dense medium and connected to a high voltage power supply. A uniform electric field perpendicular to the electrodes, where the field amplitude is $E = i_0/d$, where i_0 is the applied voltage and d is the distance between the electrodes.

The medium size TPC has a shape of a parallelepiped inscribed in a cylinder with 12 field shaped rings delimiting it, and it is sustained by four bars that are fixed to the flange, which host a number of CF flanges and feedthroughs. The anode consists of wire planes positioned with different orientations to each other thus providing the spatial resolution of the track, XY coordinate, and the Z coordinate is given by the time interval between the passage of the charged particle and the arrival of the drifting electron to the wire plane. The cathode is a metallic mesh held by two cylindrical frames as shown in Fig. 4.

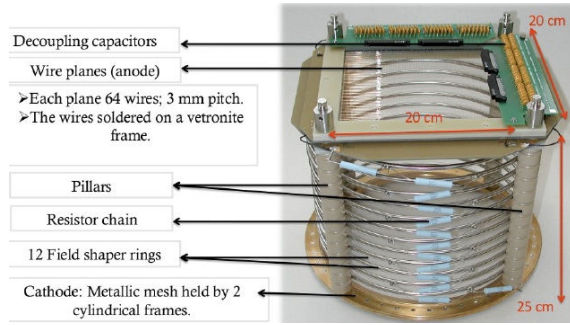


Fig. 4 Inner part of the LAr

The TPC is complemented by a photo-multiplier, PMT, immersed in LAr, which is used to trigger the system. The inner part of the detector with a TPC are contained in a stainless steel cylinder with 50cm diameter and a height of 110cm, see Fig. 5.

The outer part is a Dewar vessel with a small evaporation of LAr and excellent thermal isolation. The TPC is immersed in a highly purified LAr in a thermal contact through a stainless steel cylinder with commercial LAr in the Dewar.

II. THEORY

The production of a real Z requires that a lepton and anti lepton or quark and anti-quark interact. The center of mass of energy necessary for this is $\sqrt{s} = M_Z c^2$.

This energy is mostly reached using colliding particle beams.

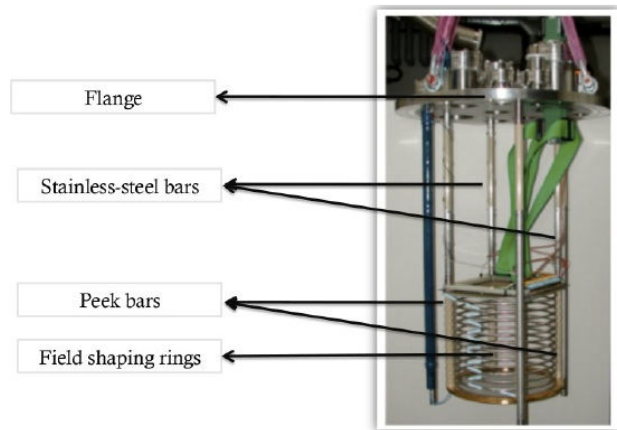


Fig. 5 LAr TPC detector

For many years the production of W and Z bosons was only possible with the help of quarks in proton beams via reactions:

$$u = \bar{u} \rightarrow q\bar{q} \rightarrow Z \quad (3)$$

Generally, we can say that in the pp collisions the Z boson is mainly produced via the annihilation of a quark and anti-quark:

$$q\bar{q} \rightarrow Z \rightarrow f^+ f^- \quad (4)$$

The intermediate boson Z is not stable; it decays to form quark anti-quark pairs and lepton-lepton pairs. The lifetime of the Z bosons is very short (10^{-26} s). The decay branching fraction of Z into quark and an anti-quark is about 70%. The branching fraction into each lepton pair channel is about 33%.

$$Z \rightarrow l^+ l^- \quad (5)$$

$$Z \rightarrow e^+ e^-, \mu^+ \mu^-, \tau^+ \tau^- \quad (6)$$

This paper shows the result of the measurement of the cross section, σ_Z in a pp collision with the center of mass energy:

$$\sqrt{s} = 14 \text{ TeV} \quad (7)$$

where the physics process is the production of a Z boson, which decay into e^+e^- final state. The experimental measurement of a cross-section is the main topic of this report. The most fundamental relationship in this measurement is the relationship between the cross section σ_Z , the luminosity, L and the rate of particle production dN/dt .

TABLE I
FORCES AND MEDIATORS

Forces	Strong	Weak	Electromagnetic	Gravitational
Mediator	Gluon, g	Z, W	Photon, γ	Graviton, G
Mass	0	91.2, 80.4	0	0
Spin	1	1	1	2

$$\frac{dN_Z}{dt} = \sigma_Z \cdot L \quad (8)$$

L is a measurement of the intensity of the proton beams; it is commonly referred to as the instantaneous luminosity, while $\int L dt$ is called the integrated luminosity. Instantaneous luminosity is usually measured in units of $\text{cm}^{-2} \text{s}^{-2}$, (1031 or 1033). Integrated luminosity is typically measured in units on inverse Pico barn (pb^{-1}) where 1 barn = 10^{-24}cm^2 . We have to address two things:

- The detector cannot record every Z boson event produced. This is called acceptance and efficiency.
- There are some events that appear as though they contain a Z , but they are really from some other process. This is called background.

Keeping these two issues in mind, the cross section will be as follows:

$$\sigma_Z = \frac{N_s - N_b}{A_Z \cdot \epsilon_Z \cdot L dt} \quad (9)$$

N_s is the number of events that contain Z boson that decay to e^+e^- , N_b is the estimated number of events in N_s that are not Z that give e^+e^- , A_Z is the acceptance, and ϵ_Z is the efficiency

in finding an interesting event.

Talking about the operating principle of LAr TPC one can say that, when a charged particle passes through the liquid argon it creates electron ion pairs along its track and UV scintillation light. The number of electrons created is proportional to the energy deposited by the ionization particles into the medium. These electrons are drifted to the sensing wires then an electric signal is provided by the readout electronics where this signal is proportional to the collected charge. We use the UV laser to calibrate the detector.

To ionize liquid argon we have to exceed the ionization potential of it, which is $\sim 14\text{eV}$, for that we need a strong beam of laser. In fact, there is no laser source with $\lambda = 89\text{nm}$ to ionize the LAr with one photon, thus we need more than one photon, and this process is known as multi-photon ionization. The Neodymium doped Yttrium Aluminum Garnet (Nd-YAG) laser with a wavelength of 266nm has proved to be applicable. The laser beam gets out from the laser head towards the next box, which contains a set of prisms to clean the beam from the residuals of the first and the second harmonic components, after which this pulse is reflected on a coated mirror then sent to clean the beam from the residuals of the first and the second harmonic components, after which this pulse is reflected on a coated mirror then sent to an attenuator then it travels through a diaphragm. This beam is then sent to a number of mirrors and later to the sensitive volume through an optical feed-through. Quartz tubes were used as an optical feed-through for the laser beam, see Fig. 6.

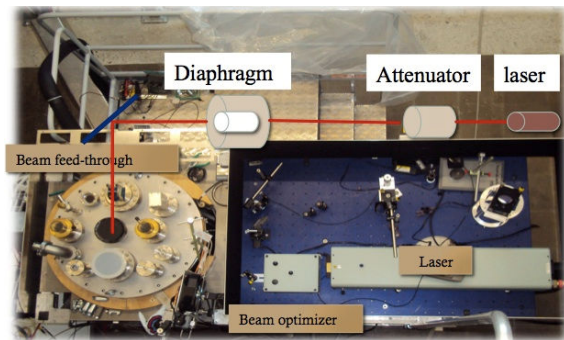


Fig. 6 Experimental setup of the laser beam

III. RESULTS

According to the reconstruction of electrons and photons in the electromagnetic calorimeter, the process chain takes place in different steps. Since the electron or the photon in the electromagnetic calorimeter deposited almost all its energy developing an electromagnetic shower, we need to reconstruct the energy of each cell of the shower, then construct a cluster of the cells, later a corrections of the energy losses in the dead matter, in the front of the calorimeter and behind are applied. A clear peak at the scale of the mass of the Z particle is a signal. For that, the Z samples that are generated are filtered at that level with a request to one fiducially lepton, electron in this case. A set of cuts had to be defined, in order to have a clear signal. In order to identify this channel we must select

events that contain two electrons, (pair of electron/ positron), that are defined in the mass window of Z boson. For electrons to be acceptable candidates for Z production both electrons need to be isolated and must satisfy the cluster shape requirement, also both electrons need to have a matching track associated with the reconstructed calorimeter cluster to separate electrons from photons and the total amount of energy that deposited in the electromagnetic cone must be greater than 90%. This will pick out the interesting electrons wanted. Furthermore, to select these electron candidates we must apply cuts to the calorimeter cluster in the event. To select the maximum number of real electrons candidates and reject as many non-electron ones, a set of criteria must be defined such as; $PT_{(e)} > 20 \text{ GeV}$, $\eta_{(e)} < 2.5$, $E_{EMCalo} / E_{HadCalo}$ is low, and that the track of the candidate particle must point to the calorimeter cluster. More cuts can be applied to ensure the selection of the events, but even after the cuts we should take into account that there is a possibility of having fake electrons. In fact, there are a number of events lost due to the kinematic cuts (PT and η), this is the Acceptance or A-geometric that is given by the following equation:

$$A_Z = \frac{N_{Z \text{ events passes PT and } \eta \text{ cuts}}}{N_{Z \text{ events}}} \quad (10)$$

Another parameter is the Efficiency which is closely related to the acceptance since both correct the number of the events lost because of the inability of the detector to record it. The efficiency is divided into two parts, the Reconstruction Efficiency and the ID Efficiency; both contribute in the identification of the lost events. In addition, it is important to identify background, which is all the particles that can mimic the electrons. Fig. 7, the reconstruction of the invariant mass of the Z decaying to e^+e^- of the signal and background, and Fig. 8, show the signal after suppressing the background with more geometric cuts applied in order to have a distinguished peak, signal. The cross section was calculated to be equal to 1432 pb with a reconstruction efficiency equal to 87% and identification efficiency equal to 89%.

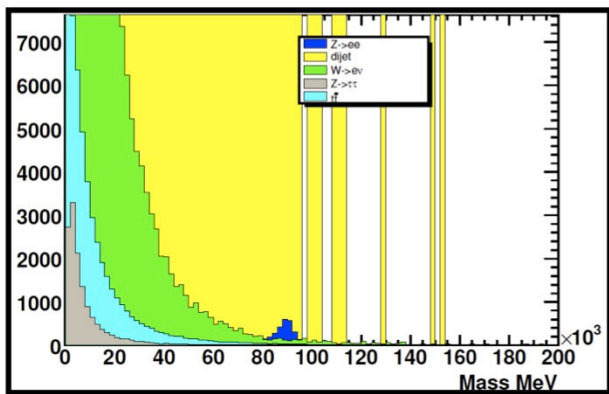


Fig. 7 The reconstruction of the invariant mass of the Z to e^+e^- of signal to background

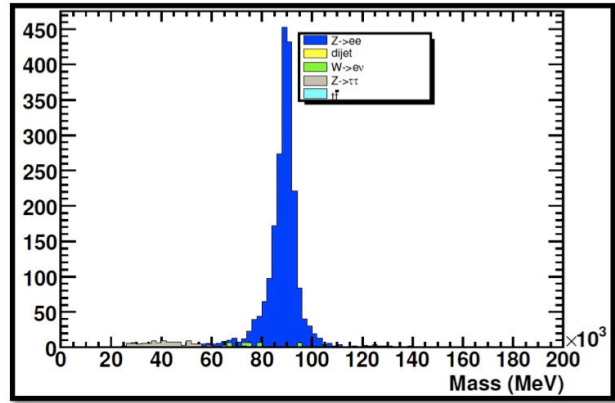


Fig. 8 More cuts applied to reconstruct and identify the mass of Z

According to the second part of the paper, in order to study the performance of the medium size LAr TPC the measurement of the purity of the LAr and consequently the electron lifetime is a key parameter in the reconstruction of the track of the ionizing particle, and for that Laser events had been used. From Fig. 9, one can see that, the lifetime (purity) increase during the time when the purification system was on, and when the system was off there was a clear decrease in the purity due to the continuous out-gassing of the detector components in the gas phase. In the last part of the plot there was some scattering in the electron lifetime and that was due to unexpected noise in the detector.

Another parameter that is important in the estimation of the number of electron yield by the ionization process is the recombination factor, which is the amount of electrons that will not be detected. The electron and ions pairs produced in the medium tend to recombine with each other unless an electric field prevents such a recombination. In Fig. 10, it is visible that the measure points scatter more than what was expected from the uncertainties associated with each point we can say that we do not see any systematic increase of the pulse height on the wires with the increase of the electric field, which is the case if there is an effect due to the recombination in the laser events.

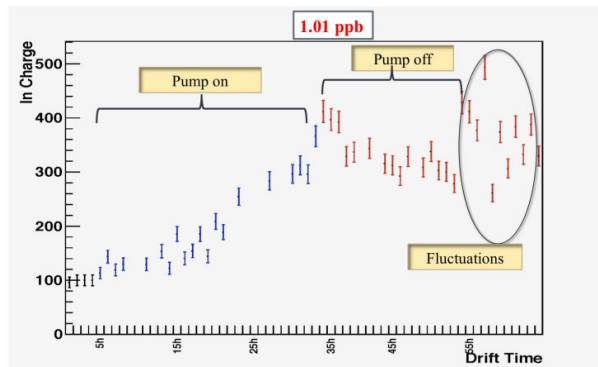


Fig. 9 The electron lifetime as function of the time showing the increase of the LAr purity using recirculation and purification systems

In fact, more studies are needed to understand the cause of the scattering while the uncertainties of the mean value of each event are not great.

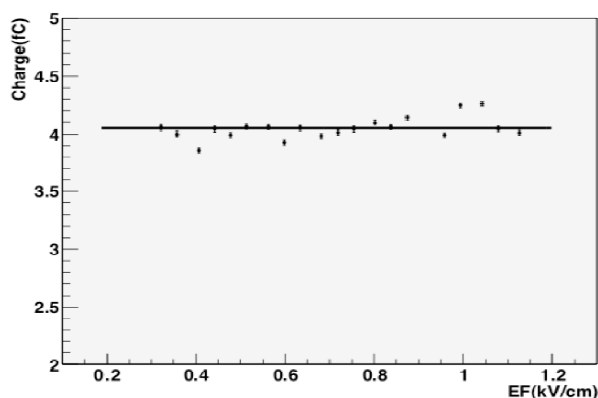


Fig. 10 The effect of recombination in the laser events

In the measurement of the cross section we measure the number of electrons created by the laser beam as a function of the photon flux. A double produced by the two laser beams produced two peaks on each wire of the collection plane. In the process of the reconstruction of the charged yielded by the second laser beam a certain number of corrections were considered, among them was the purity correction factor. Fig. 11 is a histogram in log- log scale where the X-axis represents the photon flux in the unit of $\text{photon}/\text{cm}^2 \text{ s}^{-1}$, and the Y-axis is the rate of electrons in unit $\text{electron}/\text{atoms}$. The cross section measured, σ_e , is equal to $1.24 \pm 0.10 \text{ stat} \pm 0.30 \text{ sys} \cdot 10^{-56} \text{ cm}^2$ [23], and the values obtained for the lifetime of the excited state and for σ_i which is the single photon transition cross section from the excited state to the ionization state are in consistency with the measurements provided by [24]-[26].

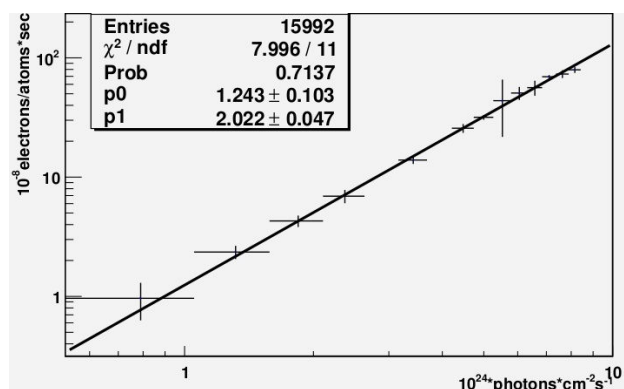


Fig. 11 Histogram the cross section of a multi-photon ionization of LAr

IV. CONCLUSION

ATLAS Experiment is one of several grand experiments on the ring of the LHC. This experiment has many channels of research in the framework of the SM and beyond, searching for new particles that explain some facts about our Universe

and others to solve puzzles and answering many unanswered questions.

The research work carried out was centered on the cross section calculation in the disintegration of the Z particle into two electrons.

A sample of data produced by a generator, then applying kinematic cuts, $\eta_{(e)} < 2.5$ and, $PT_{(e)} > 20 \text{ GeV}$, were studied looking for electrons with a Reconstructed Efficiency equal to 87%. In order to identify events efficiently more cuts were applied to the sample, thus the Identification Efficiency reached 89%. Comparing the signal to background gives a clear peak of the signal in the window of 60-100 GeV after applying kinematic and identification cuts. The cross section events of Z to e^+e^- are 1432 pb. For the low efficiency we had to work on finding why there were a loss in that value, and how to increase the effectiveness of the reconstruction and identification of the events by, for example; taking into account the electron/positron for $\eta_{(e)}$ that is higher than 2.5 and which passes through the bulk of the calorimeter.

With all the knowledge that we have today and with a clear understanding of the universe and the world around us through observations and experiments, we are still looking for answers to open questions about some particles, and their behavior. One of these particles is the neutrino, and for the detection of this elusive particle where many techniques were set to do so. The LAr TPC is one of the promising techniques that provide an excellent capability of imaging and work with a wide range of energies. Using the medium size LAr TPC gives us the opportunity to understand in-depth the multi-photon ionization of the LAr using a UV laser beam, that allows us to measure the cross section of this process.

REFERENCES

- [1] F.Hazlen, A. D. Martin: Quarks and Leptons, 1984.
- [2] D. H. Perkins: Introduction to High Energy Physics, 1972.
- [3] D. J. Griffith: Introduction to Elementary Particles, 1987.
- [4] Povh. Rith. Scholz. Zetsche: Particles and Nuclei, 1999.
- [5] The ATLAS Collaboration: ATLAS Liquid Argon Calorimeter Technical Design Report, CERN/LHCC, 1996.
- [6] Large Hadron Collider: Conceptual Design Report, CERN, 1995.
- [7] John N. Bahcall: Neutrino Astrophysics, 1989.
- [8] H. Bethe and R. Peierls, NATURE, **133**, 532, April 7, 1934.
- [9] B. Pontecorvo, Inverse process, Chalk River Laboratory, Report PD 205, 1946.
- [10] B. Pontecorvo, Sov. Phy. JETP **6**, 1958, 429.
- [11] David O. Caldwell: Current Aspects of Neutrino Physics, 2001.
- [12] Z. Maki, M. Nakagawa, and S. Sakata, Prog. Theory. Phys. **28**, 1962, 870.
- [13] J. N. Abdurashitov et al: SAGE Collaboration: Measurement of the solar neutrinos capture rate with gallium metal. III. Results for the 2002-2007 data taking period, (SAGE collaboration), Phys. Rev. C **80**, 2009, 015805.
- [14] R. Wendell et al: Atmospheric neutrino oscillation analysis with subleading effects in Super- Kamiokande I, II, III, (Super-Kamiokande Collaboration), Phys. Rev. D **81** 2010 092004.
- [15] Y. Fukuda et al: Solar Neutrino data covering solar cycle 22, (KAMIOKANDE Collaboration), Phys. Rev. Lett. **77**, 1996, 1683.
- [16] K. Abe et al: Solar neutrino results in Super- Kamiokande I, Phys. Rev. D **83**, 2011, 052 010.
- [17] B. Aharmim et al: Low energy thresholds analysis of the phase I and phase II data sets of the Sudbury Neutrino Observatory, Phys. Rev. C **81**, 2010, 055 504.
- [18] M. Apollonio et al: Limits on neutrino oscillations from the CHOOZ experiment, Phys. Rev. B **466**, 1999, 415.

- [19] A. A. Aguilar-Arevalo et al: Event Excess in the MiniBooNE search for $\bar{\nu}_e$ (MiniBooNE Collaboration), Phys. Rev. Lett. 105, 2010, 181 801.
- [20] C. Rubbia: The Liquid Argon time Projection Chamber: a new concept for Neutrino Detector, CERN-EP/77-08, 1977.
- [21] S. Amerio et al: Design, construction and test of the ICARUS T600 detector, Nucl. Instr. And Meth. A 527, 2004, 329.
- [22] J. Sun et al: Investigating laser-induced ionization of purified liquid argon in a time projection chamber, Nucl. Instrum. Methods Phys. Res. A 370 372, 1996.
- [23] I. Badhrees et al: Measurement of the two-photon absorption cross-section of liquid Argon with a Time Projection Chamber, New. J. Phys. 12 (2010) 113024.
- [24] H.J. Hilke: Detector calibration with lasers, A review, Nucl. instr. Meth. in Phys. Res. A 252 (1986) 196.
- [25] J. Bourotte and B. Sadoulet: Ionization of multiwire proportional chamber gas by double photon absorption, Nucl. Instr. Meth 173 (1980) 463.
- [26] G. S. Hurst et al: Resonance ionization spectroscopy and one-atom detection, Rev. Mod. Phys. 51 (1979) 767.